Emerging non-local quantum time correlation phenomena in a classical system of organo-metallic microparticles

I Carmeli, Vladimiro Mujica, Pini Shechter, Zeev Zalevsky

Emerging non-local quantum time correlation phenomena in a classical system of organo-metallic microparticles.

I. Carmeli, Vladimiro Mujica, Pini Shechter, Zeev Zalevsky

Abstract

We investigate enantiomers of chiral organo-metallic particles which exhibit collective memory effect. Under the influence of magnetic field, the millions of particles in solution form macroscopic shapes and when dispersed again at zero field they return to their original shape. The microparticles forming the shaped structures are collectively coupled under the influence of long-range van der Waals exchange interactions which govern the collective macroscopic structure. We recently have found that non-local quantum exchange interactions between particles persist up to ten meters, close to room temperature. Here, we investigate further the perception of time in the system. We find that the particles exhibit temporal correlations between the future and present states of the system. The forces which govern the collective memory effect and shape the macroscopic structure therefore allow to visualize quantum phenomena which extend the classical causality notion into an expanded nonlocal space-time reality. We propose that the observations are attributed to chirality-discriminating van der Waals exchange interactions coupled to vacuum fluctuations.

Introduction

Action leads to reaction and cause to effect, summarizes in short, the experience of the everyday life of the Newtonian classical world. The second law of thermodynamics states that the arrow of time points in one direction, leading to increasing entropy. However, in physics, the fundamental laws are time-symmetric: these laws predict that for every process found in nature its time-reversed version should also be possible. A definite physical and mathematical solution to the breaking of time-reversal symmetry is still an open question. However, quantum systems with weak values have been proposed to feature future events that affect the present state of the system. The notion of weak measurements involves observers which do not perturb much the quantum state of the system, an approach termed protective measurement[1]. The system is described by two (instead of one) quantum states evolving in opposite directions of time: wave function evolving toward the future and the second evolving backwards in time from a future measurement[2,3]. Weak measurements of photons[4], photon-electron interactions[5] and light interaction with plasmonic slit[6] have all proven that in weak measurements observation of the quantum system in the present is coupled to the future state of the system.

A complementary view to weak measurements is Wheeler's delayed-choice experiments[7,8]. In this experiment, the configuration of a two-path interferometer is chosen after a single-photon pulse has already entered it: either the two paths are open, and an interference is observed, or only one path remains open and the particle nature is perceived. Thus, one decides if the photon shall have come by one route or by both routes after it has already done its travel. The delayed choice determines in this case, if the single-photon exhibits wave or particle-like behavior. Experiment with single photons[9], single atom[10], photon-atom interactions[11] have proven that delayed choice will determine the outcome of such measurements. They confirm Bohr's view that it does not make sense to ascribe a wave or

particle behavior to a particle before the measurement takes place. Weak measurements and delayed choice experiments have all been performed so far on pure quantum systems such as photons, electrons and single atoms in which the quantum nature of the wave function is dominant. In this work we show that a classical system of millions of coherently coupled microparticles, exhibits nonlocal temporal correlations between the future and present states of the system.

Recently[12], we have developed a system of enantiomers of chiral organo-metallic particles with non-local quantum properties. After magnetization of the particles in solution on a 1T disk magnet overnight, the system of millions of micro-particles forms macroscopic shapes (~1cm in size) after sinking to the bottom of the container. The particles possess collective memory effect (CME), that is, under the influence of magnetic field they form macroscopic shapes and when dispersed again at zero field they return to their original shape. Although each particle is a classical microscopic particle the shape formed is governed by the quantum nature of the interactions between all particles that give rise to the macroscopic shape. The microparticles forming the shaped structures are collectively coupled under the influence of long-range van der Waals exchange interactions which govern the collective macroscopic structure. The nonlocal quantum exchange interactions between particles persists up to ten meters at temperatures above 0^0C. The CME in this system, therefore, enables visualization of quantum phenomena by the naked eye in the classical world close to room temperatures. This non-local system of microparticles grant us with the first requirement for causality to be muddled, that is, information about an object in question must become non-localized, smeared out in space instead of contained in a specific point. In the current paper, we extend the work further to the time domain and demonstrate that the system dynamics also exhibits nonlocality in time.

The organometallic microparticles

The compounds reported in this work are part of a family of diamagnetic organo-metallic composites and organized organic thin film (OOTF) on metal surfaces that possess unexpected magnetic properties. It was found that mixing molecular and metal surface electronic states in these materials can lead to new hybrid states that exhibit novel electronic/magnetic properties such as long-range coherent states, Rabi splitting, and a new type of magnetism[13–17]. Unlike regular CMR materials which are inherently magnetic due to the magnetic ions the organo-metallic compounds CMR in this case, is attributed to the unique magnetic properties of these materials which arise from the interaction of two diamagnetic compounds: the chiral molecule and the silver.

The micro-aggregates and crystals are composed of chiral and nonmagnetic organic enantiomers of Cinchonine and Cinchonidine embedded within a nonmagnetic silver (Ag) particle framework. Particles based on Cinchonine (Cin(+)), Chinchonidine (Cin(-)) and mixed compounds with equal amounts of the enantiomers (Cin(+-)) were synthesized. Image-1 shows the diverse crystal shapes and aggregates formed in the synthesis with some of the crystals demonstrating chiral shapes. We have previously shown that similar particles to those synthesized in this study exhibit chiral-dependent rotation on the water-air interface[18]. The modified synthesis of the current particles investigated has been previously described[12]. It should be stressed that all syntheses are performed at the same synthesis condition. Although the synthesis of Cin(+), Cin(-) and Cin(+-) are identical except for the chirality of the molecular enantiomer which changes, the material outcome color and composition are different as can be seen in the images of the synthesis outcome, spectroscopic data and TEM (SI.1).

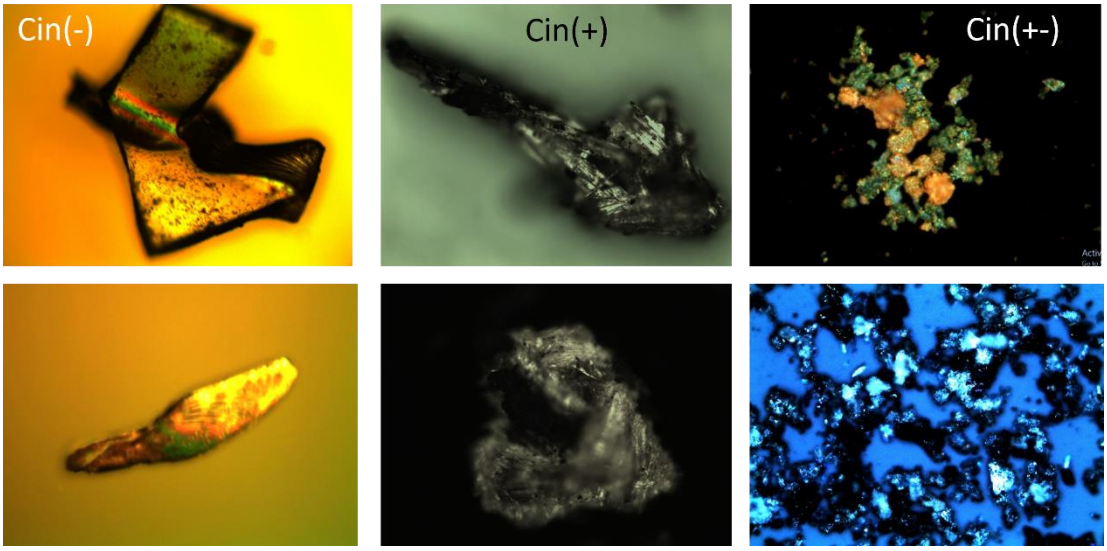

Image1: Optical images of crystal and aggregates of Cin(-), Cin(+) and Cin(+ -) particles. The particle size ranges from several microns to a couple of tenths of microns.

We have found that the macroscopic shapes formed depend on the magnetic field shape and size. For instance, a point disk magnet will result in a different CME compared to a rectangular magnet. The CME structure was very susceptible to magnetic fields as the macroscopic structure obtained aligned with the Earth's magnetic field[12]. Particles which were magnetized by a 1T in solution overnight showed positive magnetization for Cin(+) and negative magnetization for Cin(-), while Cin(+-) demonstrated intermediate magnetization properties. Strikingly, the same compounds which were not magnetized (with the 1T magnet), had opposite behavior in which the Cin(-) magnetization is higher than that of the Cin(+). The opposite magnetization is linked to opposite charging of the enantiomers by the magnetic field. Magnetization was shown to induce an opposite charging effect for cin(+) compared to cin(-) material[12]. In particular, the charge on the nitrogen in the complex of cin(+) becomes more positive after magnetization by 48% in contrary to the charge of cin(-) nitrogen which is more negative by 49% after magnetization, as determined by XPS. This dramatic effect was attributed to the influence of chirality-discriminating van der Waals interactions coupled to effective molecular spin/orbital magnetic moment. We attribute this unique magnetization behavior to induction of the positive charge and creation of an exciton band. We propose that the exciton created is stabilized by the hydrophobic interactions between the molecules and their interaction with the silver. The excitons in the molecular layer coupled to the metal form a new state of matter in which exchange interactions action at a distance are owed to long range vacuum fluctuations assisted hydrophobic interactions[12].

The non-local interactions

To study distance dependence of the collective interactions, we embarked upon various experiments adopted from the field of quantum entanglement in the following manner: 6ml of the solution particles are magnetized overnight on a 1T disk magnet. The particles are then stirred well with a pipette and split evenly into two bottles, each with ~3ml. The two bottles are separated in all cases by at least 15cm and up to 10 meters apart. The particles are left to sink to the bottom at a temperature of $6C^0$ and the shape evolution in each bottle is imaged

over several days. After shape is formed, one of the bottles (assigned b(x)) is subjected to various types of physical stimuli, such as a magnetic field or chemical induction while the second bottle (assigned b(x')) is monitored to see how modulation in b(x) has affected the organization of particles in the b(x'). In this experiment it was found that modulation of b(x) affects the shape in the twin bottle b(x') at a distance up to 10m even in cases when b(x') was shielded by Mu metal change. The distant particles (after prepared and separated as described above) were shown to be coupled even without the induction of any magnetic field and demonstrate image exchange reflection[12]. It was found that the shapes formed are not only complementary but, in several cases, also reciprocal. That is, they reflect some of the characteristics of the twin structure formed in the separated bottle.

The long-range interactions observed, can be seen as if the particles in b(x') feel the same potential as the material in b(x). It is as if they are located at the same position with no separation. The conclusion was reached after various correlations in shape formation between b(x) and b(x')[12]. One can view these results as if space, as we know it, does not exist in the trivial way we sense it. As space changes for these particles also time must change since space and time are interlinked by general relativity. The question is how time is perceived in these classical-quantum systems? It has been proposed that in organo-metallic systems time perception changes along with space and even by a larger degree on account to the strong interaction these system have with the vacuum fluctuations[19].

Temporal correlations in a macroscopic quantum system

We have tested the intriguing possibility that the particles have a correlation in time between future and present states of the system. The method was to stimuli b(x) by a magnetic field or chemically and record the response in both twin bottles to the modulation at times prior to the effect. Because we are probing the effect of time and not the effect of space between the two vials, that is, we probe future and present states of the system, the distance between the vials in these experiments is not a factor. Figure 1 below demonstrates such an experiment.

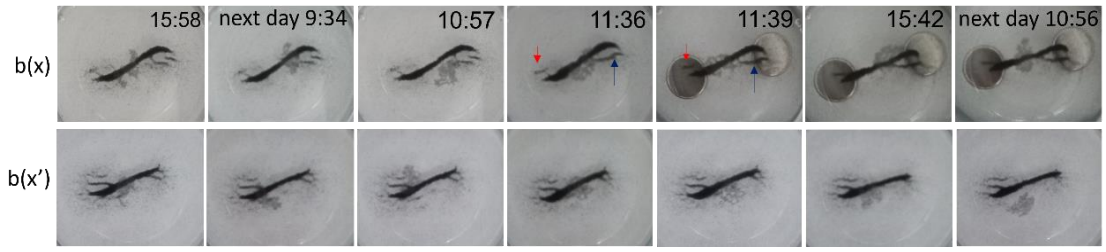

Figure 1: Temporal correlations in the organometallic particle system: Small disk magnets are inserted below b(x) at 11:39 h. The material reacts to this change 3 minutes before placement of the magnets by broadening and sending arms toward the future magnet position. The material in b(x') reacts similarly to b(x). Notice also that the material line in b(x') tilts horizontally in parallel to the tilt at 15:42 in b(x). b(x)-b(x') separation was 20cm. See also Gif of SI2 for clarification.

In this experiment, magnets were places beneath b(x) at 11:39 and the shapes in both vials were recorded starting a day before the event of magnet placement. What is seen is that three minutes before the magnetic modulation (at 11:36) the shape thickens and arms stretching toward the future magnets get more defined. b(x') changes in a similar way parallel in time to

b(x'). We can confirm that the observed changes are caused by the magnet, since several hours later the shape continues to transform, and the arms get even more defined. The Gif (SI2) depicts the sequence of events for both bottles. An additional example of similar response behavior is presented in SI3. Following magnet placement (Fig.1), small amount of acid was added to b(x) and left for two days, and subsequent base solution was added and left for two additional days (not shown) which dispersed the material in b(x) (fig.2). The dispersed material did not change for several days until 18 minutes before 2 small ball magnets were inserted into *the solution* of b(x). The insertion of the ball magnets caused the material to feel a stronger magnetic potential as described previously[12] where the ball magnets cause the material shape to conciliate and bend. The ball magnets cause the material in b(x) to start rearranging in a line between the magnets 18 minutes prior to the insertion of the magnets and cause a small bending in the material shape in b(x') parallel to the material change in b(x) at 11:25. After insertion, the material line in b(x) continues to get more defined. In this example the material felt the future potential of the magnets 18 minutes before their insertion (see Gif of SI4 for clarification). After this, the round magnet was taken out of b(x) and inserted again the following day. The absence of the magnets was preceded by the weakening of the material line in b(x) ~0.5 hours before the magnet's extraction and the insertion the next day was proceeded by the formation of a more defined line shape between the round magnets ~ 1hour before their reinsertion as seen in SI5. The changes in b(x') were in accordance with b(x) with the bending of the line in b(x') increasing at the same time a more defined line appeared in b(x), before magnet insertion. Additional example of bending of the material line prior to insertion of round magnets is presented in SI6. In this example, we can see again how the material in b(x') responds in parallel to the changes of the material in b(x).

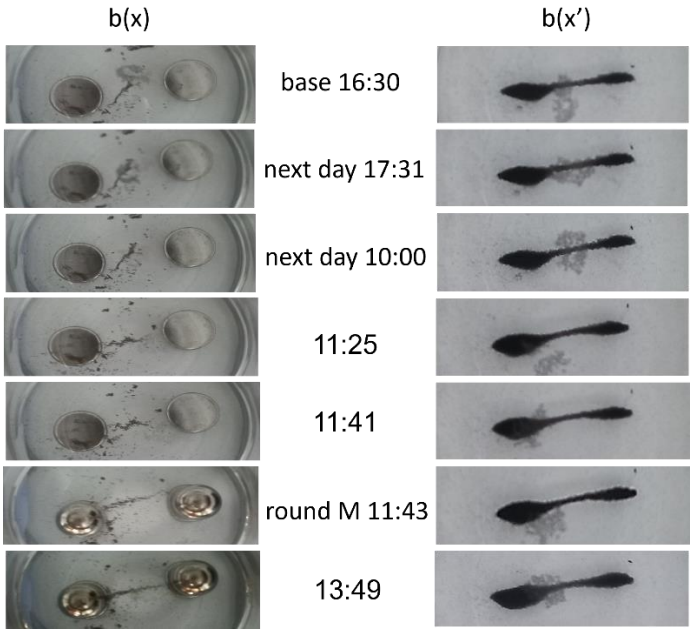

Figure-2: Insertion of small round magnets in b(x) at 11:43 h causes line arrangement of material in b(x) 18 minutes (at 11:25) before their insertion and small bending in b(x') in parallel to the change in b(x). b(x)-b(x') separation was 20cm. See also GIF of SI4 for sequence of events and focus on the bending effect.

In what follows is presented clear evidence of temporal correlations. This time the starting point was b(x) and b(x') separated by 15cm with b(x') in Mu metal cage and b(x) placed with two small disk magnets underneath the vial. Figure-3 shows that in day one the material in b(x') starts to arrange in a similar fashion to b(x). In the image b(x') the material sends arms as if grabbing the disk magnet, mimicking material is b(x). This is mostly vivid on the right arm (see also Gif.1 of SI.7). Three days the particles in b(x) and b(x') do not change until the 5th day at 10:08 in which they deform at the same time to similar forms (bottle necks on the right side). They continue to change dramatically, and images taken at 11:42 show that they transform simultaneously to more defined shapes with a tilt angle. The similarity is also vivid in the notch on the right magnet side which is seen also in b(x') right side. At 12:55 both shapes take on a more bent edgy and defined structure before the insertion of two small ball magnets inside the solution of b(x) at time 13:12. Gif.2 of SI.7 depicts the evolution of the shapes over six days. As shown previously, insertion of ball magnets into the solution of particles causes the particles to form a more organized and well-defined shape with a tilt angle and some bending, as also in this case (day 5 11:42-12:55, see also Gif.3 of SI.7 for comparison). This experiment demonstrates that the particles behave accordingly to the effect of small ball magnets insertion, however they do it prior to insertion of the ball magnets and both vials react in parallel to the insertion of the ball magnets, up three hours prior to the vent.

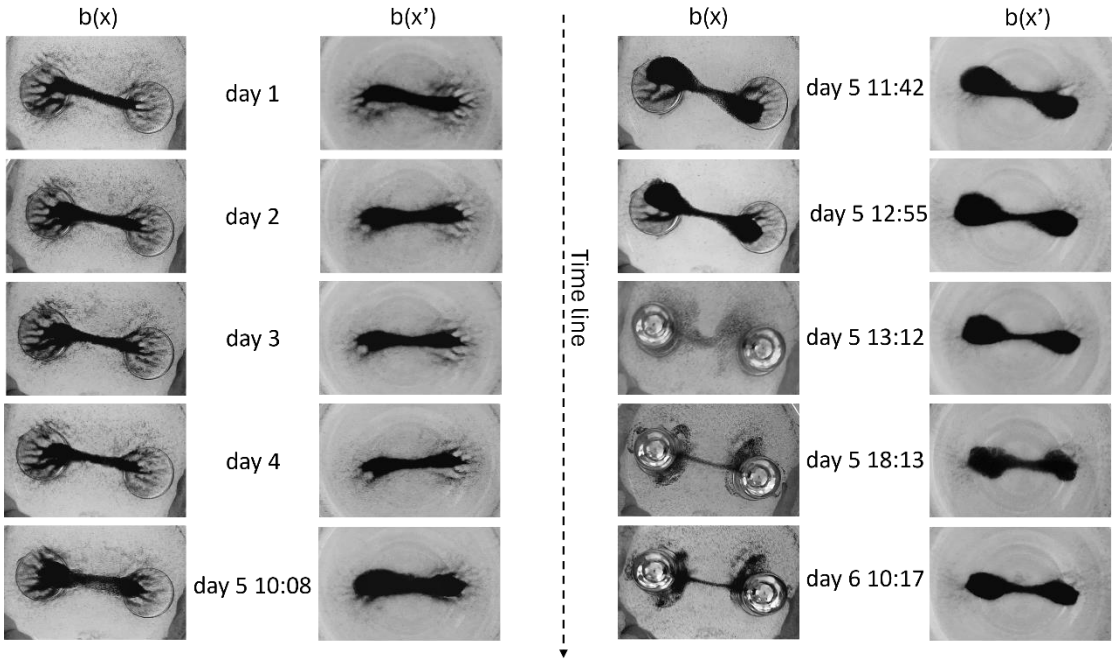

Figure-3: After three days (days 2-4) in which no change in shape is observed insertion of ball magnet into the solution at the fifth day (13:12) causes a dramatic change to a more defined line shape. The change begins ~3 hours prior to the insertion of the ball magnets and intensifies before the insertion. Notice the change in shape that occurs in parallel for b(x) and b(x') for all times up to the insertion of the ball magnets.

Day 7: the material line between the magnets in b(x) weakens and the shape in b(x') starts to show some asymmetry accumulating more material on the left side, before the ball magnets are taken out of solution at 11:30 (Fig.4 and Gif.1 of SI.8). The asymmetry intensifies for both b(x) and b(x') structures over the next two days. The two shapes take on complementary

structures with larger density distribution on the top right for b(x) and bottom left for b(x') with almost orthogonal tilt angles, day 9 – 11:42-13:49 (Gif.2 of SI.8 illustrates the large asymmetry between the shapes). At day 9 (18:01) **5** minutes prior to insertion of rectangular magnet both shapes consolidate and start to reveal facets with straighter lines. The asymmetry starts to break and material from the right bulb of b(x) starts to move left. More apparent, is the shift of material from the left bulb of b(x') toward the center, reducing the asymmetry. After insertion of the rectangular magnet (18:06) the shape in b(x') continues to consolidate and lose its asymmetry. The tendency of material migration to the right and consolidation which initiated before insertion of the rectangular magnet progress in b(x') until the asymmetry is lost (day 12). Gif.3 of SI.8 demonstrates the sequence of all the events.

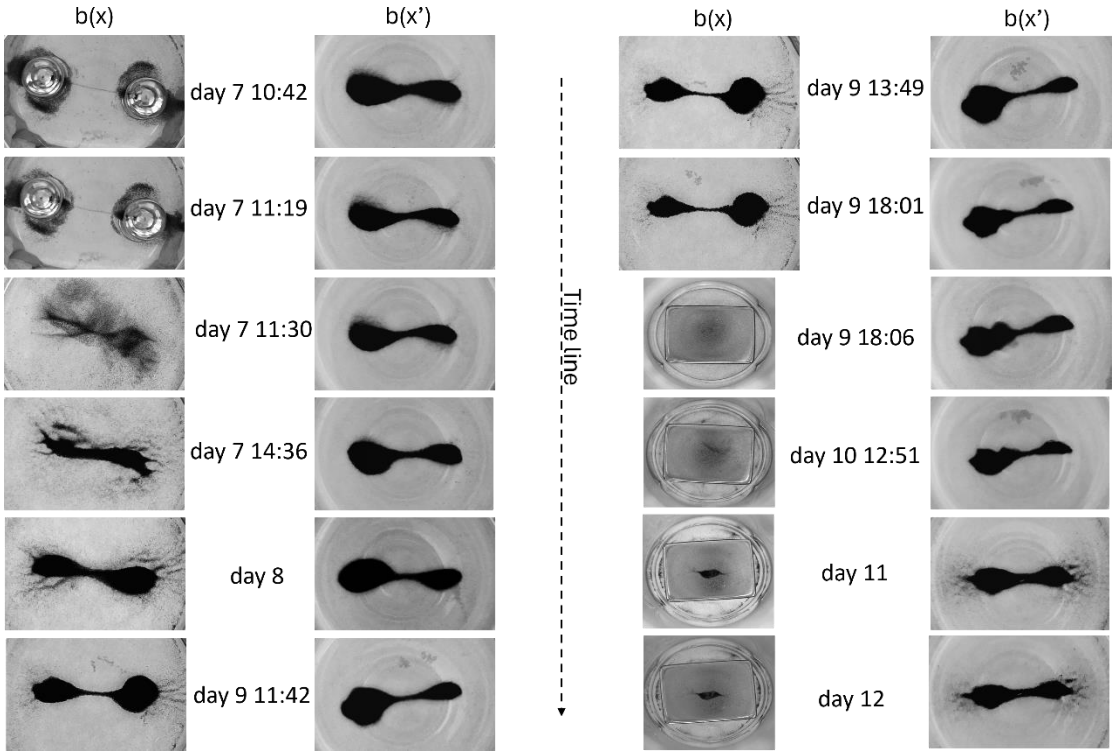

Figure-4: Sequence of events continuing experiment presented in Fig.3. The experiment demonstrates in several ways temporal correlations between future and present states of the particle system (see text and SI8 for detail).

The weakening of the material line (day-7 11:19) before removal of the ball magnets (day-7 11:30) was expected as shown in SI5. Asymmetry that begins *prior* to removal of the ball magnets, intensifies later on is manifestation of the complementary nature of the material when not subjected to any magnetic field[12]. The complementary shapes in this case are different from the one presented in reference- 12 due to the memory the material has to its previous magnetic state. There is consolidation of the structure (day-9 18:01) beginning of asymmetry breaking by material which flows from the edge of the shape toward the center (best seen in b(x') left shape side) and straight facets which start to emerge in b(x') (and seen to some degree also in b(x)) are all expected[12] from the insertion of rectangular magnet (day-9 18:06) which converts b(x') shape to a more linear defined edgy structure. This tendency which has begun prior to insertion of the rectangular magnets proceed until at day 12 in which the asymmetry is almost completely lost and the shape is linear (and not bent) as expected

from a rectangular magnet effect[12]. In all the various examples of this experiment the particles demonstrate temporal correlations between present and future states of the system.

Next, we add Sodium borohydride (4mg) to b(x) as in ref 12 and apply an external magnetic field at -45^0, $+45^0$ and then again -45^0 to the normal of b(x) for several days (not shown). This changes the magnetic response of the material, leaving the coupling of b(x)-b(x') intact, as can be seen in Fig.5 bellow (day1-14:38). The particles in b(x') take on a round shape positioned left top to the center of the vial which is in correspondence to particles in b(x) concentrating mainly around the top left ball magnet. At 11:38 day3 there is an abrupt change in the shape of b(x') particles. Part of the structure transforms to a rectangular shape. At 18:41 day3, the whole structure takes on a rectangular characteristic, centered at the middle of the vial. Particle distribution in b(x) also shift toward the right magnet, covering a wider area (see Gif of SI9). Three minutes later at 18:44 the ball magnets are replaced by a rectangular magnet. At day 4 the bottom part of the rectangular slides left and the top slides to the right (see SI10) giving a squarer form to the shape. In b(x) the particles shape also in a squarish form.

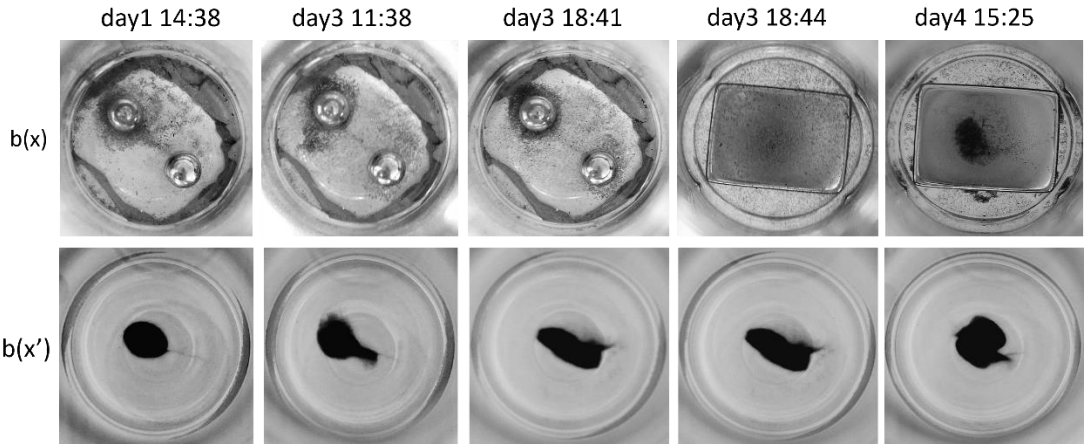

Figure-5: Sequence of events continuing experiment presented in Fig.4. Note that this time the intervals between each measurement are longer than in the previous experiment (Fig.3-4). See Gif of SI9 for sequence of events.

Two days later, day6 at 16:01 the particles still maintain a rectangular characteristic (Fig.6) with bottom and top straight facets lines. In day8 at 14:45 there is again an abrupt change in the shape in b(x'), transformation to a round shape left top to center with a remanence of the rectangular characteristic at the center of the vial. Notice that this shape resembles very much the one seen on day3 11:38. b(x) shape transforms abruptly in a similar way to b(x'). At 15:34 ~50 minutes later both shapes in b(x) and b(x') take a rounder form, top left to the center, resembling in position and shape day1. At 15:42 day8, 8 minutes later the rectangular magnet is replaced by the ball magnets.

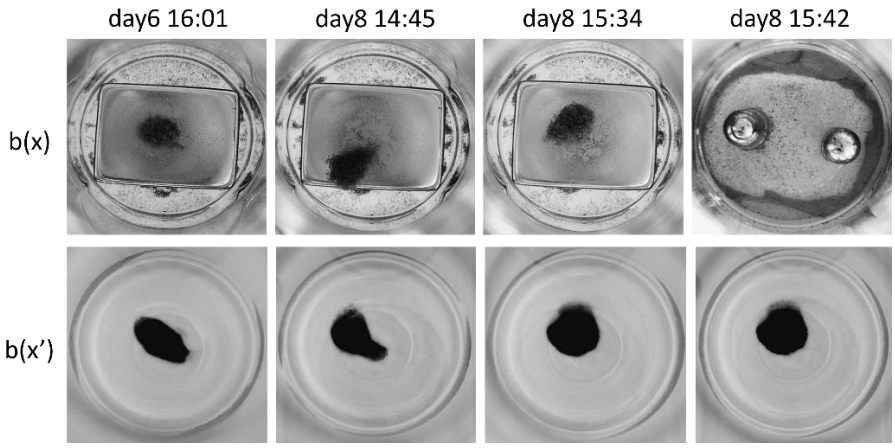

Figure-6: Sequence of events continuing experiment presented in Fig.5. See Gif of SI11 for sequence of events.

In this experiment we started with ball magnets, changed to rectangular, and then returned to the ball magnets. What is observed is that *prior* to the insertion of the rectangular magnet and then again, its replacement by the ball magnet there is an abrupt transformation in the shape of the particles which corresponds specifically to the shape of the magnet which will be inserted. Especially striking, is the similarity between the shapes (2 and 5) of Figure-7 which present the intermediate stages of each sequence. The shapes are in-between a round shape (ball magnet) and a rectangular (the rectangular magnet). In the intermediate stage (2) the round shape represents the present state and the rectangular shape, the future state of the system. In the intermediate state of (5) this is reversed. The rectangular structure represents the current state, while the round form, the future state of the system (see Fig.7).

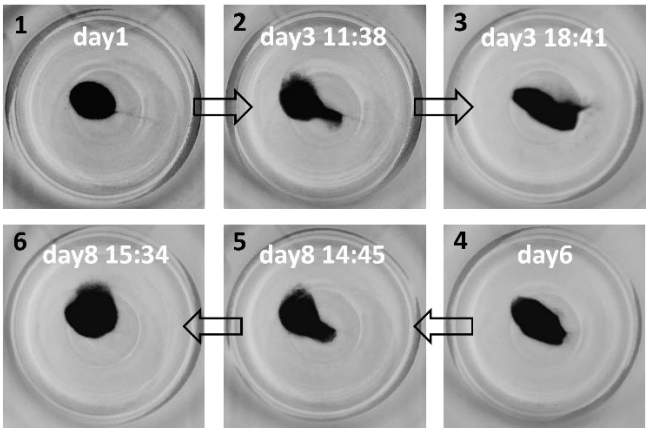

Figure-7: Presents the material state of b(x') at several stages. (1-3) *are all in which ball* magnets are still in b(x). (2-3) are before changing to a rectangular magnet in b(x). (4-6) are the inverse action (to (1-3)) of replacing the rectangular magnet (in b(x)) to ball magnets. (4-6) *are all in which a rectangular* magnet is still in b(x). (5-6) are before changing back to the ball magnets in b(x). The figure illustrates the change in shape prior to magnet replacement (2-3) and the inverse effect (5-6). Especially striking, is the similarity between the shapes (2 and 5) in the intermediate stage of each sequence. The transition form in (2) has intermediate state in-between a round shape (ball magnet-present form) and a rectangular shape (future rectangular magnet). The intermediate state (5) has intermediate shape in-between rectangular (rectangular magnet-present form) and a round shape (future ball magnets). (1)

transforms toward the center while (4) toward the upper left side. See also Gif of SI12 for alternation between modes.

We have noticed that in the second round of acid-base insertion, the particles in the solution start to change color. Following that, we test the color change before the addition of acid/base. SI13 (see also Gif) shows that the color of the particles bound to the magnets changed to yellow 3 hours before the insertion of a couple of drops of NaOH 6M base. The color continues to intensify after base addition (SI14). Two days after the color had changed to deep orange, several drops of acid (HCl-6M) were added at time 13:18. An ~hour and a half before acid insertion the color of the particles starts to fade, and this tendency continued after acid insertion until the magnets return to their original color (SI14 and Gif1). In addition to the color fade, the line of material between the ball magnets gets less defined before acid insertion and the material moves away from the center where the acid drops will be added (SI14 and Gig1). Material shape in b(x') responds to acid addition in b(x) by bending half an hour before acid insertion to b(x). This bending is best seen at time 13:16, 2 minutes before acid is added (Gif2 of SI14). The bending effect is typical to acid addition[12].

SI15-17 presents three more examples in which material clears the position where acid/base drop is added, prior to its insertion. This behavior is contrary to the insertion of magnets which strengthen the material line as seen in Fig.2-3 and previously reported[12].

The material can also shape itself in the image of the magnet placed inside the solution several hours before insertion of the magnet as shown in Fig.8. The ball magnet placed inside the solution of particles is taken out and replaced after two days by a rectangular magnet. The material that was in round shape for two days changed shape to rectangular, ~1:20 hours before the insertion of the rectangular magnet. The full sequence of events is presented in SI18 and Gif. An additional example of pre-shape change is presented in SI19.

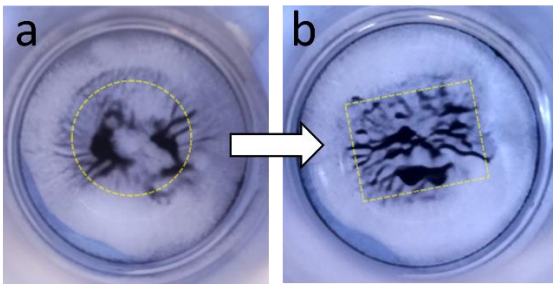

Figure 8: Particles after a ball magnet that was placed inside the solution was taken out (a) and replaced after two days by a rectangular magnet. The material that was in round shape for two days(a) changes shape to a rectangular shape (b) ~1:20 hours before insertion of the rectangular magnet (the insertion is not shown). The full sequence of events is presented in SI18.

We have performed time dependent XPS measurements to get more confirmation for temporal correlations on an atomic level. The events chosen were insertion of Acid/Base, based on their observed effects on the particles[12] and their big effect to change the Nitrogen charge of the molecules in the compound. The experiments are performed by taking for XPS analysis small amount (10µl) of material from the vial at different times (from several days down to one minute) prior to application of a future activation event. Material is also taken for analysis after application of the event. In these experiments we have confirmed that temporal correlations between future and present states of the system, exist on an atomic

level. That is, we observe changes in charging of the Nitrogen atom and changes of the silver peak prior to insertion of Acid/Base. The XPS results and their interpretation are given in SI.20-21.

Discussion

Recently, we reported on the observation of CME phenomena in a large assembly of organo-metallic microparticles. Experiments proved that the millions of particles are coupled in a coherent manner to each other. When two systems of particles are separated their chirality is in a complementary state which is governed by long distance exchange interactions. We attribute the ability to observe quantum phenomena to the CME effect and its forces which act to couple millions of particles into one entity with coherent properties, given rise to a macroscopic shape which can be viewed by the naked eye. The exchange interactions between the distant particles, creates an actual force which moves the particles so that they will organize in a complementary way to each other. The two systems of particles were shown to display image exchange and experience the same potential (magnetic/chemical) applied on the distant particles, as if they were located at the same position with no separation. The non-local interactions were accounted to quantum fields of particles in b(x), that occupy the same "space" as particles in b(x') although they are separated by a distance of up to ten miters. One can view these results as if space, as we know it, does not exist in the trivial way we sense it. As space changes for these particles also time must change since space and time are interlinked by general relativity. The question is how time is perceived in these classical-quantum systems. In the past it was proposed, that in organo-metallic systems time perception changes along with space and even by a larger degree on account to the strong interaction these system have with vacuum fluctuations[19].

Molecular self-assembly on metal surfaces forms a new excitonic band[20,21]. Correlation was found between the exciton band and reduction in Casimir forces[22]. This suggests that surface charges interact with vacuum fluctuations. The exciton band gives rise to a new type of magnetism when diamagnetic chiral molecular films are self-assembled on diamagnetic metal surfaces[13,19]. We have proposed[12] that the exciton is created and stabilized by the hydrophobic interactions between the molecules and their interaction with the silver. The excitons in the molecular layer coupled to the metal form a new state of matter in which exchange interactions at a distance are owed to long range vacuum assisted hydrophobic forces. The possible existence of a nonlocal effects in quantum systems similar to the ones observed in the organometallic system is supported by several recent theories. The transfer of angular momentum through the vacuum fields has been recently proposed[23] and the exchanges of conserved quantities could occur even across a region of space in which there is a vanishingly small probability of any particles (or fields) being present[24]. The energies associated with this might be thought to be very high, however, recent theories has suggested that quantum materials such as Weyl semimetals[25] can break classical conservation lows due to quantum vacuum fluctuations[26,27] and that quantum particles can possess very high energies in a process of time-holistic, double non-conservation effect which yet still obeys the standard conservation laws[28].

In the present work, we showed that the system of microparticles demonstrates correlations in time, between the future and present states of the system. It is proposed that the particles

are doing so, by non-local exchange interactions in the time domain, in a similar way to their non-local exchange interaction in space. The notion of two separate positions in space and two separate points in time does not exist for the particles. Pauli exclusion principles state that identical particles under exchange must have opposite spins. We propose a second exclusion principle, which states that identical particles that exchange in the time domain (between present and future) must have opposite charges. We propose that the exciton obeys this condition by having a positive and negative charge as a same unit that permits nonlocal expansion in time as in space. It is interesting to note that the CME is strongest at low (6C) temperatures. At RT the shapes formed are dispersed. It has been shown that at temperature close to 0^0C the positive and negative charges of the exciton equals[19,29] creating a resonance. This suggests that this charge equalization might be a criterion to obey the exclusion principle in the time domain.

The phenomena observed in this work can be viewed as caused by collective exchange interactions between the state of the particles in non-local space and time regime. The forces which govern the collective memory effect and shape the macroscopic structure therefore allow to visualize quantum phenomena which extend the classical causality notion into an expanded nonlocal space-time reality.

References:

1. Aharonov, Y. & Vaidman, L. Protective Measurements of Two-State Vectors. in *Potentiality, Entanglement and Passion-at-a-Distance* 1–8 (Springer, Dordrecht, 1997). doi:10.1007/978-94-017-2732-7_1.

2. Aharonov, Y. & Vaidman, L. A New Characteristic of a Quantum System between Two Measurements — A "Weak Value". in *Bell's Theorem, Quantum Theory and Conceptions of the Universe* 17–22 (Springer, Dordrecht, 1989). doi:10.1007/978-94-017-0849-4_3.

3. Aharonov, Y. & Vaidman, L. Properties of a quantum system during the time interval between two measurements. *Phys. Rev. A* **41**, 11–20 (1990).

4. Realization of a measurement of a ``weak value''. *Physical Review Letters* https://journals.aps.org/prl/abstract/10.1103/PhysRevLett.66.1107 (1991) doi:10.1103/PhysRevLett.66.1107.

5. Pan, Y. *et al.* Weak measurements and quantum-to-classical transitions in free electron–photon interactions. *Light Sci Appl* **12**, 267 (2023).

6. Weak Measurements of Light Chirality with a Plasmonic Slit. *Physical Review Letters* https://journals.aps.org/prl/abstract/10.1103/PhysRevLett.109.013901 (2012) doi:10.1103/PhysRevLett.109.013901.

7. Quantum Theory and Measurement. in *Quantum Theory and Measurement* (Princeton University Press, 2014).

8. *Quantum Theory and Measurement*.

9. Jacques, V. *et al.* Experimental Realization of Wheeler's Delayed-Choice Gedanken Experiment. *Science* (2007) doi:10.1126/science.1136303.

10. Manning, A. G., Khakimov, R. I., Dall, R. G. & Truscott, A. G. Wheeler's delayed-choice gedanken experiment with a single atom. *Nature Phys* **11**, 539–542 (2015).

11. Dong, M.-X. *et al.* Temporal Wheeler's delayed-choice experiment based on cold atomic quantum memory. *npj Quantum Inf* **6**, 1–7 (2020).

12. Carmeli, I. *et al.* Emerging non-local quantum phenomena in a classical system of organo-metallic microparticles. *arXiv.org* https://arxiv.org/abs/2412.17553v1 (2024).

13. Carmeli, I., Leitus, G., Naaman, R., Reich, S. & Vager, Z. Magnetism induced by the organization of self-assembled monolayers. *The Journal of Chemical Physics* **118**, 10372–10375 (2003).

14. Dintinger, J., Klein, S., Bustos, F., Barnes, W. L. & Ebbesen, T. W. Strong coupling between surface plasmon-polaritons and organic molecules in subwavelength hole arrays. *Phys. Rev. B* **71**, 035424 (2005).

15. Canaguier-Durand, A. *et al.* Thermodynamics of Molecules Strongly Coupled to the Vacuum Field. **125**, 10727–10730 (2013).

16. Hernando, A. *et al.* Giant magnetic anisotropy at the nanoscale: Overcoming the superparamagnetic limit. *Phys. Rev. B* **74**, 052403 (2006).

17. Carmeli, I. *et al.* Tuning the critical temperature of cuprate superconductor films with self-assembled organic layers. *Angew Chem (Int Ed Engl)* **51**, 7162–7165 (2012).

18. Carmeli, I. *et al.* Unidirectional rotation of micromotors on water powered by pH-controlled disassembly of chiral molecular crystals. *Nat Commun* **14**, 2869 (2023).

19. Carmeli, I. Time Expansion at the Interface of Organic Metallic Surfaces. *AIJR Preprints* (2022) doi:10.21467/preprints.411.

20. Carmeli, I. The Effect of Spin on Photoelectron Transmission through Organized Organic Thin Films. (2003).

21. Neuman, O. & Naaman, R. New Optical Absorption Band Resulting from the Organization of Self-Assembled Monolayers of Organic Thiols on Gold. *J. Phys. Chem. B* **110**, 5163–5165 (2006).

22. Sedmik, R. I. P., Urech, A., Zalevsky, Z. & Carmeli, I. Efficient Reduction of Casimir Forces by Self-Assembled Bio-Molecular Thin Films. *Advanced Materials Interfaces* **11**, 2400365 (2024).

23. Xu, H. *et al.* Non-Hermitian Spin-Spin Interaction Mediated by Chiral Phonons. *arXiv.org* https://arxiv.org/abs/2411.14545v2 (2024).

24. Aharonov, Y., Collins, D. & Popescu, S. Angular Momentum Flows without anything carrying it. *arXiv.org* https://arxiv.org/abs/2310.07568v6 (2023) doi:10.1103/PhysRevA.110.L030201.

25. Gooth, J. *et al.* Experimental signatures of the mixed axial-gravitational anomaly in the Weyl semimetal NbP. *Nature* **547**, 324–327 (2017).

26. Kim, I. H., Shi, B., Kato, K. & Albert, V. V. Chiral Central Charge from a Single Bulk Wave Function. *Phys. Rev. Lett.* **128**, 176402 (2022).

27. From Entanglement Generated Dynamics to the Gravitational Anomaly and Chiral Central Charge. *Physical Review Letters* https://journals.aps.org/prl/abstract/10.1103/PhysRevLett.129.260403 (2022) doi:10.1103/PhysRevLett.129.260403.

28. Aharonov, Y., Popescu, S. & Rohrlich, D. Conservation laws and the foundations of quantum mechanics. *arXiv.org* https://arxiv.org/abs/2401.14261v1 (2024) doi:10.1073/pnas.22208101201of9.

29. Carmeli, I., Gefen, Z., Vager, Z. & Naaman, R. Alternation between modes of electron transmission through organized organic layers. *Phys. Rev. B* **68**, 115418 (2003).

Author Information

Itai Carmeli: University Center for Nanoscience and Nanotechnology and Department of Materials Science and Engineering, Tel Aviv University, Tel-Aviv 69978 and Faculty of Engineering, Bar-Ilan University, Ramat-Gan 52900, Israel.
Vladimiro Mujica: School of Molecular Sciences, Arizona State University, Tempe, 85287-1604, Arizona, USA.
Pini Shechter: Jan K Department of Material and Interfaces, Weizmann Institute, Rehovot 76100, Israeloum Center for Nanoscience and Nanotechnology Tel-Aviv University, Ramat-Aviv, Tel-Aviv, 6997801, Israel
Zeev Zalevsky: Faculty of Engineering, Bar-Ilan University, Ramat-Gan 52900, Israel.

Link to SI: https://doi.org/10.6084/m9.figshare.28179362.v1

Materials

XPS measurements

X-ray Photoelectron Spectroscopy (XPS). XPS measurements were performed using a Thermo Scientific ESCALAB QXi. The samples were irradiated with a monochromatic Al Kα radiation. High resolution spectra were collected with a 20 eV pass energy. Spot size measurements was 650 µm in diameter.

TEM

Tunneling electron microscopy images taken by scanning and transmission electron microscope ((S)TEM), equipped with a Schottky-type S-FEG (standard-shape field emission gun) that produces a high-stability electron beam. TEM contrast images and electron diffraction patterns are recordable by a Ceta-M camera that may yield 3 frames per second at an outstanding resolution of 4096px x 4096px. STEM bright and dark field micrographs are recordable by a segmented PANTHER detector (4 BF x 4 DF segments) that offers the option for contrast enhancement by DPC and iDPC techniques (differential phase contrast and integrated DPC).